Modulation of Photon Echo Intensities by Ultrasonic Waves in Ruby and Alexandrite

D. Boye, W. Grill, J. E. Rives, and R. S. Meltzer

Department of Physics and Astronomy, University of Georgia, Athens, Georgia 30602
(Received 23 May 1988)

Modulations of the intensity of two-pulse photon echoes due to ultrasonic waves are described for alexandrite and ruby. Enhancements (up to a factor of 8) of the echo intensity are observed. The main features of the echo intensity changes are well described by a model in which the ultrasonic waves modulate the optical transition frequencies of the echo-producing Cr^{3+} ions effecting a spatially dependent phase accumulation which compensates for the phase mismatch.

Generally, when an ensemble of coherently excited ions in a solid interact with vibrational excitations, the ion-vibration interaction perturbs the optical transition frequencies of the individual ions in a stochastic manner producing a pure dephasing. In this case, the transition frequency shifts induced by the strain are spatially uncorrelated. However, if the vibrational excitation is coherent, the modifications of the phase relationships of the excited ions are spatially correlated, as discussed in a recent paper by Wilson, Wackerle, and Fayer[1] in which they propose an experiment to detect coherent optical phonons and to measure electronic excitation-phonon coupling matrix elements. In this paper we present experimental evidence for the predictions of Wilson, Wackerle, and Fayer for the case of coherent ultrasonic waves rather than high-frequency optical phonons. We demonstrate that for ultrasonic waves, where the strain is coherent over the full sample length, the ion-vibration interaction can lead to both reduction *and,* when phase matching is incomplete, enhancement of photon-echo intensities (PEI). Modulations of PEI have been routinely seen as a result of superhyperfine effects,[2] and intensity modulations of spin echoes have been observed as a result of pulsed electric fields.[3] However, to the best of our knowledge, this represents the first experimental evidence for modulations of optical coherent transient signals by acoustic waves. PEI and spin-echo intensity enhancements have been previously achieved either by the use of the multiple-pulse Carr-Purcell echo-train technique,[4] or in the two-pulse arrangement under the condition of constant pulse delay with the technique of nuclear spin decoupling[5] to lengthen the dephasing time, T_2. We believe that this is the first example in which PEI enhancement has been produced using a two-pulse technique at constant T_2. This effect can be used to measure the ion-phonon coupling, provide sensitive detection of acoustic waves internally within a sample, and to enhance photon-echo signals when spatial-phase matching is incomplete.

We describe photon-echo experiments in alexandrite (0.054 at.% Cr) and ruby (0.018 at.% Cr) at $T = 1.5$ K in which the PEI is modulated by rf acoustic waves, ob-

tained from a 0.2-mm-thick $BaTiO_3$ ceramic transducer attached to the sample with a thin layer of low-temperature epoxy. The echo is obtained on the $^4A_2$, $-\frac{3}{2} \rightarrow {}^2E(\bar{E}, -\frac{1}{2})$ transition of Cr^{3+} in a 30-kG magnetic field, $H \parallel a$ $(H \parallel c)$ for alexandrite (ruby). The two polarized $(E \parallel b$ for alexandrite, $E \perp c$ for ruby) pulses used to prepare the coherence are obtained from a single Nd-doped yttrium-aluminum-garnet pumped tunable dye laser with an optical delay line and are focused to a 300-μm-diam spot. They have pulse energies of 20 and 80 μJ, a bandwidth of 0.3 cm^{-1}, and a temporal width of 5 ns. Rejection of the scattered laser light is accomplished spatially, with a crossed-beam excitation geometry (2° crossing angle), and temporally, with a Pockels cell. Because of the long optical path lengths in the samples used in these experiments (0.6 mm in alexandrite and 6 mm in ruby), phase matching is incomplete. The acoustic waves modify the phase-matching condition by producing a spatially dependent phase accumulation which compensates the phase mismatch. The result is a PEI which depends on the relative timing of the preparation pulses with respect to the phase of the acoustic wave.

An example of the PEI modulation effect in alexandrite is shown in Fig. 1. A pair of piezoelectric transducers, separated by about 0.5 mm to allow passage of the laser beams, are attached to the sample as shown in the upper left of Fig. 1 so that longitudinal acoustic waves can be propagated along the direction of the light beams by our driving the transducers with an rf voltage source (longitudinal geometry). The PEI is measured as a function of the time, t_0, between the zero phase of the rf voltage source (defined in the upper right inset of Fig. 1) and the first of the echo preparation pulses, labeled as pulse 1. It is observed that the PEI modulations, which have zero amplitude in the absence of the imposed acoustic waves, always occur at the rf driving frequency and that their amplitudes show strong enhancements at the acoustical resonances[6] of the sample consisting of the crystal and attached transducers (multiples of 4.45 MHz). The dependence of the PEI modulations on the rf voltage, V_{pp}, is shown in the left column of Fig. 1 for a

    © 1988 The American Physical Society
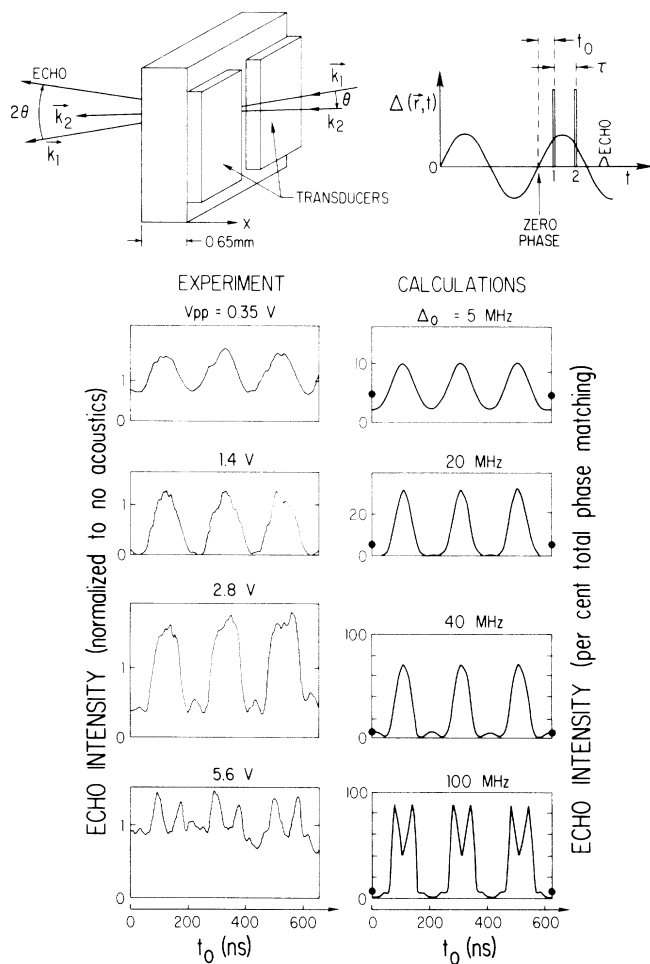
FIG. 1. Experimental and calculated PEI modulations in alexandrite for 4.45-MHz rf excitation and $\tau = 20$ ns. The experimental data are shown for several peak-to-peak voltages, V_{pp}, applied to the piezoelectric, and are normalized to the echo intensity in the absence of the ultrasonics. The calculations are those obtained for different amplitudes of the acoustically induced frequency shift, where Δ_0 is the amplitude of the frequency shift at an antinode of the stress. The dots indicate the PEI calculated without acoustics. Upper left: Geometry of the experiment showing the 0.2-mm-thick $BaTiO_3$ piezoelectric transducers attached to the sample and the echo preparation pulses 1 and 2 of wave vector k_1 and k_2. Upper right: Timing of optical pulses 1 and 2 and the echo relative to the phase of the acoustic wave which produces a transition frequency shift, $\Delta(r,t)$ at position r in the sample.

rf frequency of 4.45 MHz. As V_{pp} is increased, the PEI modulations first deepen and then modulations with higher harmonics appear.

PEI modulations which occur at the acoustic period, T, are also observed when acoustical pulses are propagated perpendicular to the light beams (transverse geometry). The PEI modulation amplitude is a maximum when $\tau = T/2$. In this geometry, enhancements of up to a factor of 8 are observed. When $\tau = T$, the modu-
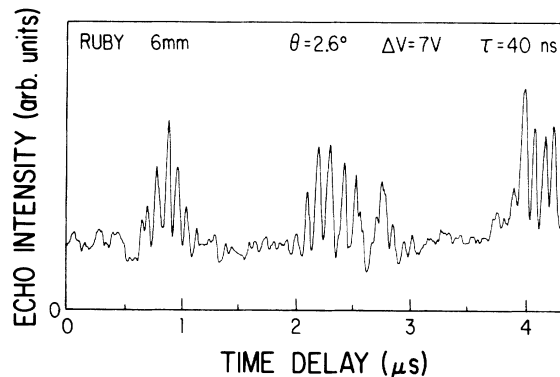
FIG. 2. Observed PEI modulations in a 6-mm-long ruby crystal due to an ultrasonic wave packet excited by the application of a $\Delta V = 7$ V 50-ns pulse to a pair of piezoelectric transducers in the same geometry as shown in Fig. 1.

lations disappear since the preparation pulses and echo all occur at the same phase and amplitude of the acoustic wave.

In a second experiment conducted in a 6-mm-long ruby sample, a 50-ns-long voltage pulse, of magnitude ΔV, is applied to a pair of piezoelectric transducers attached as in Fig. 1. As the acoustical wave packet, consisting of about five oscillations, arrives near the central 2 mm of the crystal (interaction region) where maximum beam overlap occurs, strong PEI modulations (mostly enhancement) are observed, as seen in Fig. 2, until the wave packet has traversed the interaction region. However, multiple reflections of the acoustical wave packet are detected, as indicated by the repetition of echo modulation episodes.

In order to identify the mechanism of the PEI modulations we first estimate the magnitude of the acoustically induced strain. We obtain this, using as a calibration, the well-known stress-induced frequency shift of the R lines in ruby[7] and alexandrite.[8] After burning a 1-MHz optical hole in the R_1 absorption line of alexandrite with a single-frequency dye laser, the laser frequency is shifted by 20 MHz with an electro-optic modulator in the cavity. The modulation of the transmitted laser light[9] is then monitored as the acoustic wave, propagating perpendicular to the optical beams so that the acoustic phase front is nearly constant over the hole-burned volume, traverses the region of the sample containing the hole. It is found that a 5-V pulse to the transducer produces about a 30-MHz frequency shift, which corresponds to an acoustically induced strain of 10^{-6}.

Possible mechanisms for the PEI modulation include acoustical alterations of the optical wave vector or of the position of the ions between pulse 1 and the echo. Calculations of the acoustical changes in either the bulk refractive index or effects associated with the R-line anomalous dispersion indicate that strains of 10^{-4} to 10^{-5} are required to explain the size of the echo intensity modula-
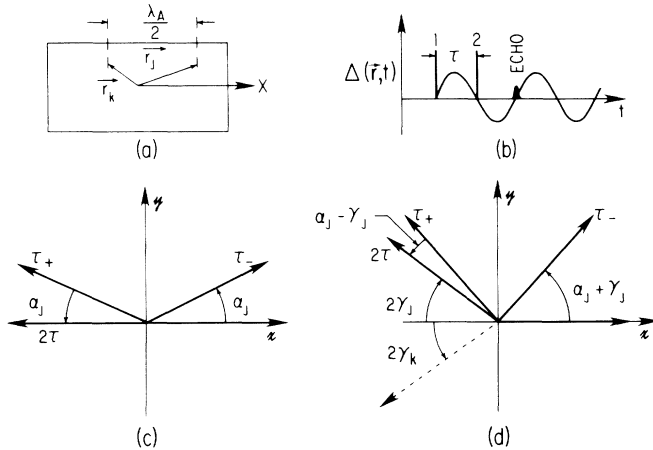
FIG. 3. Schematic showing the phase accumulation of the Bloch vector in the rotating frame. (a) The sample showing the acoustic wavelength. (b) The timing of the optical pulses and echo relative to the acoustic wave which would produce the maximum phase accumulation. (c) Time evolution of the Bloch vector in the absence of acoustics. (d) Time evolution of the Bloch vector for an ion at position r_j in the presence of the acoustical pulse shown in (b).

tions. A similar result applies to acoustical modulations of the ion positions. Since the measured strains of 10^{-6} are 1 to 2 orders of magnitude smaller, we turn to temporal effects.

Acoustically induced optical transition frequency shifts which are position dependent can lead to a spatially dependent phase accumulation which can compensate for the phase mismatch. Effects of phase accumulation due to electrically induced transition frequency shifts have indeed been observed for spin echoes.[3] The prediction by Wilson, Wackerle, and Fayer[1] that coherent optical phonons can reduce the photon-echo intensity depends on just this effect. The situation is represented in Fig. 3 with an xy-plane projection of the Bloch vector in the rotating frame (rotation frequency v_0, taken as the center of the inhomogeneous line). Consider an atom, j, seen in Fig. 3(a), located in the sample at position r_j, whose optical transition frequency is shifted from the center of the inhomogeneous line by an amount $v_j - v_0$. In the absence of the acoustic wave, the optical pulse 1 rotates the Bloch vector from the $-z$ axis to the x axis as shown in Fig. 3(c). At the beginning of pulse 2 at τ_-, the Bloch vector has rotated by an angle a_j. Pulse 2, which ends at τ_+, produces a $180°$ rotation about the y axis, the pseudospin axis of the light. At time 2τ, the Bloch vector has again advanced by an angle a_j so that it lies along the $-x$ axis for all ions, independent of the transition frequency. As a result, a macroscopic dipole moment develops generating the echo.

Consider the effect of an idealized acoustic wave at which r_j develops a positive optical frequency shift, $\Delta(r_j, t)$, between pulses 1 and 2 and a negative frequency

shift between pulse 2 and the echo, as shown in Fig. 3(b). At time τ_-, just before pulse 2, the Bloch vector has experienced an additional positive phase accumulation, γ_j, at τ_- as shown in Fig. 3(d). The second pulse, ending at τ_+ again produces a $180°$ rotation about the y axis. During the time interval, τ, between pulse 2 and the echo formation, the Bloch vector acquires a phase angle $a_j - \gamma_j$ so that the Bloch vector lies at an angle of $-2\gamma_j$ from the $-x$ axis. For an atom k, located at r_k, half an acoustic wavelength along the X axis from atom j, the phase accumulations are just opposite in sign to that of atom j. As a result, its Bloch vector lies at an angle $2\gamma_j$ from the $-x$ axis, also shown in Fig. 3(d). Consequently, there occurs a spatially modulated phase accumulation which partially compensates for the spatial phase mismatch.

The PEI is calculated as described by Abella, Kurnit, and Hartmann[10] from

$$I \propto |\ \{\exp[i(k_1 - 2k_2 + k) \cdot r + i\gamma(r)]\}_{av}\ |^2 , \qquad (1)$$

where the average is performed over the sample volume determined by the overlap of the two crossed preparation pulses. The PEI modulations in alexandrite, for the longitudinal geometry, are calculated for the case of a standing wave whose wavelength is twice the length of the crystal and the transducer, corresponding to the 4.45-MHz resonant frequency of the sample in the fundamental mode.[6] In this mode the end of the alexandrite crystal attached to the transducer is approximately at an antinode and the opposite end is at a node of the stress.

To obtain the phase accumulation, γ, we use the expression of Wilson, Wackerle, and Fayer,

$$\gamma(r)/2\pi = -\int_0^\tau dt\, \Delta(r,t) + \int_\tau^{2\tau} dt\, \Delta(r,t) , \qquad (2)$$

where in this case the amplitude of the frequency shift is spatially dependent on the coordinate, X (colinear with k_2). The expression for the frequency shift for a crystal of length, L, is

$$\Delta(r,t) = \Delta_0 \cos[\tfrac{1}{2}\pi(X/L - 1)]\sin[2v_A(t + t_0)] , \qquad (3)$$

where Δ_0 is the amplitude of the frequency shift at an antinode, t_0 defines the phase of the acoustic wave at the time of pulse 1, and v_A is the acoustic frequency. The transducer is attached at $X = L$.

The calculated PEI as a function of time is shown on the right column of Fig. 1 for several values of Δ_0 for the case $\tau = 0.1T$ (20 ns), consistent with the conditions of the experiments with which they are compared in Fig. 1 (left column). For small Δ_0 (corresponding to small V_{pp} on the transducer) the calculated modulations are at the acoustic frequency and exhibit both enhancements and reductions in intensity, consistent with the experiments. As Δ_0 is increased (values selected in proportion to V_{pp} for comparison to the experiments), additional modulations with higher-frequency components appear. Note the strong similarity to the observed pattern of modulations. The amplitude of the frequency shifts required to

produce the observed modulation depths are in the range of 10–100 MHz, which is in agreement with measurements based on hole burning. However, the large magnitude of the PEI enhancements predicted in the calculations for $\Delta_0 > 20$ MHz are not observed. The most likely explanation is that deviations of the acoustic wave from plane-wave phase fronts produce significant reductions in the echo enhancements, especially for large strains where relatively small spatial variations can lead to important relative frequency shifts across the sample. Heating by the rf transducer power may also reduce the enhancements at large V_{pp} by phonon-induced stochastic-dephasing processes.

Calculations of PEI modulations for a pulsed wave packet consisting of four oscillations have also been performed in an attempt to qualitatively simulate the experimental results in ruby presented in Fig. 2. The experimentally observed deep-echo modulations, with large intensity enhancements, are also seen in the calculations when the wave packet enters a 2-mm-long section of the sample chosen so as to imitate the interaction region in the center of the sample. As Δ_0 is increased, conditions of near total phase matching are predicted yielding enhancement factors of 10. Enhancement factors of more than 3 are observed (Fig. 2).

We conclude that ultrasonic waves are capable of producing large effects on the PEI, including enhancements in crossed-beam geometries, because of an acoustically induced phase accumulation which is spatially dependent. Observable modulations should occur with frequency shifts as small as 100 kHz, making this an extremely sensitive detector of acoustic waves. In addition, it provides a new method for measuring the coupling of elastic waves to electronic excitations. These effects should be observable in many different types of coherent-transient experiments. Indeed, we have observed strong attenuation of optical-free induction decay signals by ultrasonic waves. The effects described here are quite general. It should be possible to produce these PEI modulations with any perturbation which produces a spatially dependent transition frequency shift during the time between coherence preparation and detection.

[1]W. L. Wilson, G. Wackerle, and M. D. Fayer, J. Chem. Phys. **88**, 3407 (1988).

[2]L. Q. Lambert, Phys. Rev. B **7**, 1834 (1973).

[3]W. B. Mims, Phys. Rev. **133**, A835 (1964).

[4]*Laser and Coherence Spectroscopy*, edited by J. I. Steinfeld (Plenum, New York, 1978), Chaps. 3 and 4.

[5]R. M. Macfarlane, C. S. Yannoni, and R. M. Shelby, Opt. Commun. **32**, 101 (1980).

[6]M. Niksch and W. Grill, Acoustica **64**, 26 (1987).

[7]E. Feher and M. D. Sturge, Phys. Rev. **172**, 244 (1968).

[8]W. Jia, Y. S. Shang, R. M. Tang, and Z. Y. Yao, J. Lumin. **32**, 272 (1984).

[9]A. L. Huston and W. E. Moerner, J. Opt. Soc. Am B **1**, 349 (1984).

[10]I. D. Abella, N. A. Kurnit, and S. R. Hartmann, Phys. Rev. **141**, 391 (1966).